Surface & Coatings Technology 422 (2021) 127540

Contents lists available at ScienceDirect

Surface & Coatings Technology

journal homepage: www.elsevier.com/locate/surfcoat

An investigation of the effect of surface characterization on Saos-2 cell proliferation after coating of titanium alloy surfaces by a selective laser melting process

Emin Orkun Olcay [a], Ayse Ercan [b], Selin Oncul [b], Ozge Arifagaoglu [c], Bahadir Ersu [d,*]

[a] Department of Prosthodontics, Faculty of Dentistry, Biruni University, 34020 Istanbul, Turkey
[b] Department of Biochemistry, Faculty of Pharmacy, Hacettepe University, 06100 Ankara, Turkey
[c] Department of Prosthodontics, Faculty of Dentistry, Baskent University, 06490 Ankara, Turkey
[d] Department of Prosthodontics, Faculty of Dentistry, Hacettepe University, 06100 Ankara, Turkey

ARTICLE INFO

Keywords:
Titanium dental implant
Ti6Al4V alloy
Ti6Al4V ELI alloy
Saos-2
Osseointegration

ABSTRACT

Pure titanium alloys are commonly employed in construction of dental implants, given their advantageous features including resistance to corrosion, mechanical strength, flexibility, and bioavailability. The purpose of this study was to evaluate the surface characteristics of Ti6Al4V alloy disks upon sand-blasted, large-grit acid-etching, and/or selective laser melting applications and to assess whether and how these surface modifications affect the attachment, viability, metabolic activity, and osteoblastic differentiation of Saos-2 osteosarcoma cells. We manufactured Ti6Al4V alloy disks and divided them into four groups (non-treated, SLA-treated, Ti6Al4V ELI alloy-coated (SLM treated), and SLM+SLA-treated). The topographic analysis was carried using AFM and SEM and chemical content was evaluated by EDX. EDS. Adherence and viability of Saos-2 cells seeded onto disks were investigated via SEM and fluorescent microscopy. To assess the metabolic activity of Saos-2 cells, MTT assay was conducted and the osteoblastic differentiation interpreted via monitoring alkaline phosphatase activity. According to data acquired using AFM and SEM, the control group had the smoothest surfaces, with a lower Ra value. The roughest surface was obtained with SLM and SLA dual-treated disks. The osteoblastic activity of Saos-2 cells on the surface of dual-treated disks was higher than the other groups. Therefore, the surface of SLM+SLA-treated disks conferred a suitable environment for Saos-2 cells to adhere, proliferate, and show higher metabolic activity. We concluded that Ti6Al4V alloy disks covered with Ti6Al4V ELI alloy and subjected to SLA surface treatment may be promising to manufacture dental implants with improved adaptability, bioavailability, and osseointegration.

1. Introduction

Tooth loss due to various factors including trauma, developmental defects, periodontitis, cavities, genetic disorders, and certain diseases is a prevalent event that may be treated with different approaches (dentures, bridges, dental implants, etc.) [1]. In past years, the industry and clinical application of dental implants have developed remarkably, improving the mechanical/chemical characteristics and biocompatibility of the implants [2]. Osseointegration, a term coined by Ingmar Brånemark, refers to the success of the integration of the implant to the bone and durability under normal physiological conditions [3]. It can take weeks or months for complete bone regeneration associated with the dental implant since the process comprises releasing of various growth/differentiation factors within the proximity of the implant, bone regeneration, and bone remodeling [4]. Additionally, corrosion, improper modulus of elasticity match, low mechanical strength, possible fractures, biological loss [5], cytotoxic/pro-inflammatory/carcinogenic effects of the implant [6], usage of certain agents such as anti-resorptive drug (ARD) and antidepressants [7,8], and consumption of tobacco [8], not to mention the physiological condition of the individual [7] influence the competence of the implantation.

Currently, pure titanium and its various alloys are used in orthopedic and dental implant construction due to the outstanding mechanical and physical characteristics of titanium [9]. Amongst these, Ti6Al4V alloys are frequently employed for biomedical applications, especially orthopedic and dental implants, by virtue of their suitable mechanical

* Corresponding author.
E-mail address: bersu@hacettepe.edu.tr (B. Ersu).

https://doi.org/10.1016/j.surfcoat.2021.127540
Received 10 April 2021; Received in revised form 17 July 2021; Accepted 20 July 2021
Available online 24 July 2021

strength [10]. Ti6Al4V, also known as Ti Grade 5, is an alpha-beta titanium alloy that is constructed with aluminum (alpha stabilizer) and vanadium (beta stabilizer) [11]. On the one hand, the low density of aluminum is expedient and it provides a tenacious structure against high temperatures [11]. Vanadium, on the other hand, is a beta-isomorphous element that accommodates a more ductile beta phase at high temperatures during construction [12]. Despite its low density, the fatigue resistance of Ti6Al4V, and its notable resistance to corrosion, make it one of the most utilized titanium alloys in diverse fields, including the aerospace industry and clinical applications [13]. Ti6Al4V extra low interstitials (ELI) (Ti Grade 23) alloy resembles Ti Grade 5, although the latter includes low levels of oxygen, nitrogen, carbon, and iron [14]. This feature of ELI aids enhanced ductility and fracture toughness and demonstrates high biocompatibility when compared with Ti Grade 5 [15]. Ti Grade 23 is also amongst the most commonly used titanium alloys in medical practice [16].

Previously, it was demonstrated that a modification of the dental titanium implant surface by specific treatments alters healthy cell attachment and proliferation, osseointegration, and wettability [17]. Since the quality, durability and bioavailability of the implants largely depend on its surface, research is focusing on improving the construction of the titanium and titanium alloy implants via different techniques such as selective laser melting (SLM) [18], plasma spraying [10], sand-blasted, large-grit acid-etching (SLA) [19], dual-acid etching (DAE) [20], grit blasting [21], and hydrothermal treatment [10].

In our study, we used Ti6Al4V alloy disks, treated with either SLA, SLM (Ti6Al4V ELI alloy-coated) or both processes. We analyzed the composition and the topography of the disks and employed the Saos-2 human osteogenic sarcoma cell line to investigate the proliferation of the cells and the osteoblastic capacity of the disks. We hypothesized that the adoption of both SLA and SLM methods to modify of the titanium alloy disks would reinforce the attachment and proliferation of the cells on the material due to increased roughness and osteoblastic capacity of the disks.

2. Materials and methods

2.1. Production of Ti6Al4V alloy disks

A Ti6Al4V alloy bar with a diameter of 6 mm was processed at 10,000 turnover/min, using a computer numerical control (CNC) lathe machine (Hanwha, XP16S, South Korea), and 48 disks with a thickness of 2 mm were obtained. The disks were rinsed with distilled water, using a pressurized vapor steamer device (Gazella Gold Dental Steam Cleaning Robot, Turkey). The final constructs were divided into four groups: untreated with any surface alteration techniques (group 1), to be subjected to SLA (group 2), to SLM (group 3), or to both of these methods. The groups are illustrated in Fig. 1.

2.2. SLA treatment of the disks

The titanium sample surfaces in groups 2 and 4 were sand-blasted using 30 μm Al_2O_3 particles (F240, Kuhmichel Abrasiv GmbH, Germany) at 6 bar pressure for 20 s. Pre-washing of the disks was done using an ultrasonic cleaning device (Wattson, Turkey), first with pure acetone (Sigma-Aldrich, USA), then with 96% ethanol (Merck, USA), and finally with distilled water, for 15 min at 80 °C. The acid etching procedure was carried out under American Society for Testing and Materials (ASTM) criteria. Briefly, the disks were acid-etched with 48% H_2SO_4 (Merck, USA) at 80 °C for 20 min and with 18% HCl (Merck, USA) at 80 °C for 20 min. Neutralization was carried out by applying 27% $NaHCO_3$ (Merck, USA) for 10 min and rinsing with distilled water. Subsequently, the samples were once more acid-etched with 8% HNO_3 (Merck, USA) at 80 °C for 20 min and neutralized with 27% $NaHCO_3$ for 10 min. The final products were again washed with distilled water. Prior to the in vitro experiments, the titanium alloy disks were placed in an ultrasonic bath, sonicated for 30 min, and exposed to ultraviolet (UV) light for 40 min to remove any organic residue.

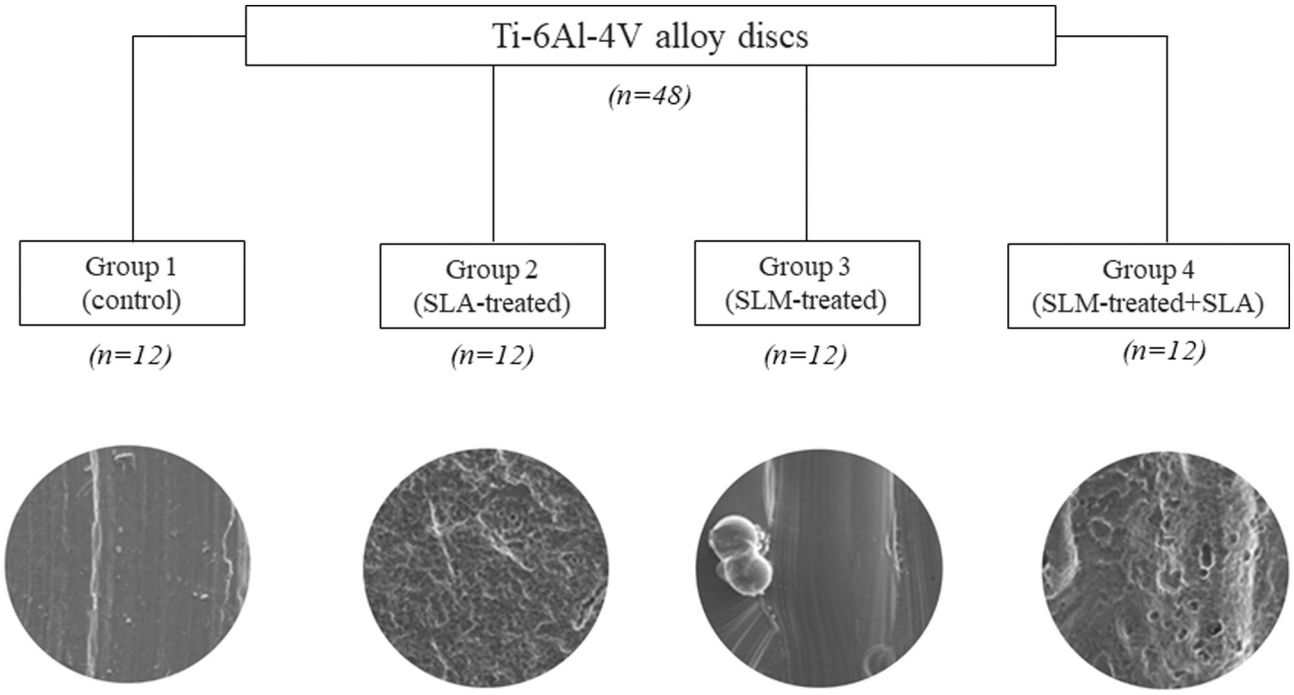

Fig. 1. The surface treatment groups of Ti6Al4V titanium alloy disks. Group 1 was not subjected to any treatment and was considered the control. The SLA method was applied onto the surface of Group 2. Group 3 was coated with Ti6Al4V ELI. The disks of group 4 were covered with Ti6Al4V ELI alloy and subjected to SLA treatment. SLA: sand-blasted, large-grit acid-etching; SLM: selective laser melting; Ti6Al4V: Titanium-6-Aluminum-4-Vanadium.

2.3. SLM application to the surface of the titanium alloy disks

The surfaces of the titanium disks in groups 3 and 4 were both subjected to SLM. Additionally, group 4 samples were subjected to SLA as well. Firstly, a stainless-steel platform was constructed corresponding to the original size of the LaserCUSING® SLM device (Concept Laser, Hofmann Innovation Group, Germany). Grooves on the sample surfaces, were fabricated on the platform. With a scanning speed of 7 m/h and a production speed of 2-20 cm^3/h, the surfaces of the titanium disk samples were coated with Ti6Al4V ELI alloy, approximately 60 μm thick. After the sintering process, the samples were kept in distilled water at 25 °C for 5 min to remove surface residues. Later, the samples were rinsed with NaOH (20 g/L) (Sigma-Aldrich, USA) and H_2O_2 (20 g/L) (Sigma-Aldrich, USA) for 30 min at 80 °C. The final samples were incubated in distilled water for 5 min. Before the in vitro experiments, the constructs were sonicated for 30 min in an ultrasonic bath and exposed to UV light for 40 min to eliminate any organic residue.

2.4. Topographic analysis of the titanium alloy disks using atomic force microscope (AFM)

A sample from each group was chosen randomly and fixed on metal trays. High-resolution three-dimensional (3D) images of the surfaces of the disks were captured using an AFM (Veeco MultiMode V, USA). Images of 40 μm, 20 μm, 5 μm and, 1 μm areas were recorded for each sample selected from the groups. The contactless method, which is based on the approach that the needle never touches the surface, was used during measurement. The distance between the probe and the sample was set to 0.5–2 nm.

2.5. Cells and culture conditions

The Saos-2 human osteosarcoma cell line (ATCC® HTB-85™) was obtained from American Type Culture Collection (ATCC). The cells were maintained in Dulbecco's Modified Eagle Medium (DMEM) supplemented with 10% fetal bovine serum, 1% 200 mM L-glutamine, 100 U/mL penicillin, and 100 μg/mL streptomycin, which were all purchased from Gibco (USA). The cells were kept at 37 °C in a humidified incubator (Panasonic MCO-18 AC-PE, Japan) supported with 5% CO_2.

2.6. Investigation of Saos-2 cell attachment and morphology on the titanium disks by scanning electron microscopy (SEM)

To analyze the surface topography of the treated groups and to compare the differentiation of Saos-2 morphology, a Scanning Electron Microscope (SEM) was used. Titanium disks from each group were placed in a 96-well plate and Saos-2 cells were seeded at a density of 1×10^4 cells/well. After 7 days of incubation, the cells attached to the surfaces of the disks were fixed with 4% glutaraldehyde (Sigma-Aldrich, USA) for 6 h. Following dehydration with increasing percentages of ethanol (Sigma-Aldrich, USA) (50% to 90% for 10 min), the cells were further adhered to the surface with hexamethyldisilazane (HMDS) (Sigma-Aldrich, USA) for 30 min. The specimens were sputter-coated with gold-palladium and the cells were examined at magnifications of 1000- and 5000-fold using a 1.2 nm high-resolution scanning electron microscope (QUANTA 400F Field Emission, USA). Additionally, energy-dispersive x-ray spectroscopy (EDX) was used aiming to qualitatively and quantitatively determine the chemical composition of each titanium alloy disk.

2.7. Imaging of Saos-2 cells on the titanium disks by fluorescent microscopy

Carbocyanin DiI dye, known for its highly lipophilic properties, was used for the fluorescent imaging of the cells. 15 μL of fluorescent DiI dye was added to a Saos-2 cell suspension (5×10^5 cells/well) and the cells were incubated for 60 min at 37 °C. The labeled cells were seeded into 6-well plates and each group of the disks was placed in individual wells. The imaging was performed with a fluorescence microscope (Zeiss Examiner A1, Germany) after 7 days of incubation. Images of the surfaces of the samples under 10× and 40× magnification were captured and qualitatively analyzed.

2.8. MTT assay

The metabolic activity of the Saos-2 cells seeded onto the titanium disks with specific surface properties was explored via MTT assay to obtain an indication of the viability of the cells on the disks. The cells were seeded on the Ti disks placed into 24-well cell culture plates (5×10^4 cells/well). After 72 h, the disks were transferred to a 96-well plate and a 5 mg/mL MTT solution was added to each well, to be incubated for 4 h. The formazan crystals formed from MTT via the dehydrogenases of viable cells were dissolved using 23% (v/v) sodium dodecyl sulphate (SDS) and 45% (v/v) dimethylformamide (DMF). Absorbance was measured at 590 nm using a plate reader (Biotek, PowerWave XS, US). The cells seeded on those disks not subjected to any surface modification applications (group 1) were considered to be 100% viable and the viability of the cells planted on the titanium alloys subjected to SLA or/and SLM were compared accordingly.

2.9. Evaluation of the alkaline phosphatase (ALP) activity of Saos-2 cells

Saos-2 cells were seeded onto the titanium alloy disks placed into the wells of a 96-well plate (5×10^4 cells/well). At the end of the 72-h incubation period, the ALP activity of the cells was measured by carrying out a colorimetric ALP assay (Sigma-Aldrich, USA). A magnesium-containing diethanolamine reaction buffer and a 0.67 M *p*-nitrophenyl phosphate (pNPP) solution were added into wells of a sterile 96-well plate. The plate was equilibrated to 37 °C and the media of the samples were transferred into this plate. The kinetic reaction based on the conversion of pNPP, a colorless compound, to p-nitrophenol, a yellow-colored compound, by ALP was monitored for 30 min at 1 min intervals at 405 nm using a spectrophotometer. The relative ALP activity of the cells seeded on the disks with distinct surface modifications was measured using the following equation:

$$ALP\ activity\left(\frac{U}{mL}\right) = \frac{\left[\left(\frac{\Delta A405nm}{min}\text{sample} - \frac{\Delta A405nm}{min}\text{blank}\right) \times \text{total volume}\right]}{18.5 \times \text{sample volume}}$$

where 18.5 is the mM extinction coefficient of pNPP at 405 nm.

2.10. Statistical analysis

SPSS and Graphpad Prism 8 software programs were used for statistical analysis of the data obtained. The difference in the ALP levels of the treatment groups at 72 h was determined by Welch variance analysis and a binary comparison Tamhane test. A Student *t*-test was carried out to conclude whether or not the viability of the cells on the disks with modified surfaces diverged from the viability of the cells on the control (group 1). *p*-Values <0.05 were considered to be statistically significant.

3. Results

3.1. Roughness of the titanium alloy disks with surface modifications

The roughness of the surfaces, surface areas, and maximum height and depths of the untreated Ti6Al4V alloy disks (group 1), or the disks subjected to SLA (group 2), SLM (group 3), or both of the techniques (group 4) were investigated via AFM. The surface morphologies of the disks indicated the variability of the different structures following the surface recast. The smoothest surface was detected on the disk of group

1. The SLA and SLM treatments, on the other hand, led to visible irregularities and a wavy structure on the titanium; something more evident on the disk treated with both SLA and SLM methods. Even with the increased magnification, the surface of the disk belonging to group 1 was observed to be the smoothest, compared to the surface of the disks of groups 2, 3, and 4. Following the SLA treatment, the surface of the disk appeared to be serrated; meanwhile, the SLM process produced a rougher surface with vertical indents. The microspheres (scaled to 100 and 20 μm, respectively) on the surface of the disk, observed after the SLM procedure, were presumably caused by oxidized titanium alloys, and occurred after melting. When the disks were subjected to both SLA and SLM procedures, the horizontal flatness and intense roughness on the surface of the titanium alloy disk became more conspicuous. This combined effect led to a more pronounced roughness, not only in comparison to the control group but also to the groups treated separately with SLM or SLA. The Ra values for one sample from each group were found to be 143, 415, 235, and 477 nm for groups 1, 2, 3, and 4, respectively. The coarsest surface was observed with group 4, with a Ra value 3.3-fold higher than the value of the disk belonging to group 1. The images regarding the topographical analysis of the disks and the graphic for the Ra values of each group are presented in Fig. 2.

3.2. Chemical composition of the disks

EDX spectroscopy was performed to examine the chemical composition of the titanium alloy disks subsequent to different surface applications. The percentages of Ti, V, Al, and O_2 are listed in Table 1. Ti and V content of group 2, subjected to SLA, were seen to be higher. In group 4, V and Al values slightly decreased compared to group 1; in concurrence, the amount of O_2 increased.

3.3. Saos-2 cell adherence on the Ti6Al4V alloy disks with specific surface properties

SEM imaging and EDX measurements were performed by randomly selecting one sample from each group. In SEM, the images of each sample were recorded at 1000 and 5000 magnifications (Fig. 3). The attachment and the morphology of the Saos-2 cells disk seeded onto the disks with different surface topographies were investigated by SEM. The Saos-2 cells on the disk group 1 disk appeared to be spherical and quite distinct from their characteristic silhouette (Fig. 4a and e). The distinctive lamellipodia formation of Saos-2 cells was visible in the SLA (Fig. 4b and f), SLM (Fig. 4c and g), and SLA+SLM (Fig. 4d and h)-treated groups. Due to the rough and coarse surfaces of the disks belonging to groups 2, 3, and 4, the general shape and grown osteoblast-like phenotype of the Saos-2 cells seeded onto them were maintained. The cell adherence on the group 4 disk was more pronounced.

3.4. Inspection of Saos-2 cells attached on the titanium disks with fluorescent microscopy

The viable Saos-2 cells attached to the modified Ti6Al4V alloy disks were examined with a fluorescent microscope. Since the group 1 disk had a relatively smooth surface with a low Ra value, the number of Saos-2 cells adhered to the surface of the disk was lower than those subjected to SLA, SLM, or the combined treatment. The cells on the SLA-treated titanium disks (group 2) were mainly located on the vertically arranged rough surfaces, as expected, and displayed a more intense proliferation than the cells attached to the disk samples in group 1. The pitted regions on the surface of the SLM-treated disks (group 3) proved easy for the Saos-2 cells to attach to and proliferate in large quantities. Application of both SLM and SLA methods on the disks (group 4) further improved this phenomenon of clusters of cells settling on the rough and horizontal faces of the disks. These findings were in keeping with the results obtained by SEM. The fluorescent microscopy images are displayed in Fig. 5.

3.5. Proliferation of Saos-2 cells on the titanium disks

When the 72-h data was analyzed, it was seen that the metabolic activity of the Saos-2 cells that had proliferated on the titanium alloy disks complied with the roughness of the sample surfaces as expected (Fig. 6a). The lowest level of activity was observed on the disks of group 1 whilst the dual surface modification of the group 4 disks contributed to the adherence, viability, proliferation and, implicitly, the metabolic activity of the cells.

3.6. ALP activity of cells attached to the surface of titanium alloy disks

The incubation of the Saos-2 cells on the titanium alloy disks with high surface roughness showed increased osteogenic differentiation and maturation of the cells, since ALP is a biochemical marker of these two cellular events (Fig. 6b). On the one hand, the group 1 disk failed to provide a milieu for Saos-2 cells to differentiate and maturate properly. On the other hand, the cells seeded onto the disks belonging to group 3 and group 4 reflected a higher ALP activity.

4. Discussion

During the last century, the rapid development of implant dentistry has paved the way for its employment in different procedures including replacement of teeth, complete-arch reconstructions, bridge formation, and intervention in maxillofacial defects [22]. Titanium and titanium alloys are commonly used as orthopedic and dental materials since they have superior properties in regards to being stable [23], resistant to corrosion [13], biocompatible, and contributing to successful osseointegration [24]. Despite these exceptional qualities, certain setbacks exist, such as titanium-related allergy or toxicity [25], the titanium alloy implant offering a surface for the formation of a biofilm [26], peri-implantitis [27], and triggered inflammatory response due to metallic debris from the implant (periprosthetic osteolysis) [25], that may interfere with the performance of the implant. Thus, various coating techniques and surface alterations to titanium and titanium alloy dental implants have been developed to improve the adaptability of the implant while minimizing impediments [28].

In this study, we constructed Ti6Al4V alloy disks, divided them into four groups, and subjected them to different surface modifications to assess their surface characteristics, chemical composition, and contribution to the attachment/proliferation of cells. The first group was not exposed to any surface treatment; the second and the third groups were subjected to SLA and SLM techniques, respectively. Group 4 was treated with both SLM and SLA methods.

The SLA method is based on erosion of a construct by blasting the surface with large-grit alumina particles followed by treatment with strong acid [29]. This treatment leads to macroroughness and micropits that ultimately increase the stability/durability of the implant, besides improving bioactivity and osseointegration [30]. The SLA technique is commonly chosen for its superior effects such as treatment predictability and small amount of time required for osseointegration and cell attachment, not to mention the reduced necessity for bone augmentations for individuals with bone density deficiency [31]. SLM, entails the construction of metal compounds with complex 3D structures out of powder [32]. Basically, using computer-aided design (CAD), a focused laser beam delivers the intended information for each construct slice into a bed of metallic powder that melts and solidifies under thermal energy exposure. Following scanning, the samples are re-coated with the metallic powder [33]. This method is relatively simple to use for surface modifications, and is frequently employed for the construction of dental implants [34].

AFM and SEM analysis data indicated that the topography of the surface of the Ti6Al4V alloy disks varies greatly following the application of different techniques. The titanium alloy blocks in group 1 were not subjected to either SLA or SLM; hence, the smoothest surface, with

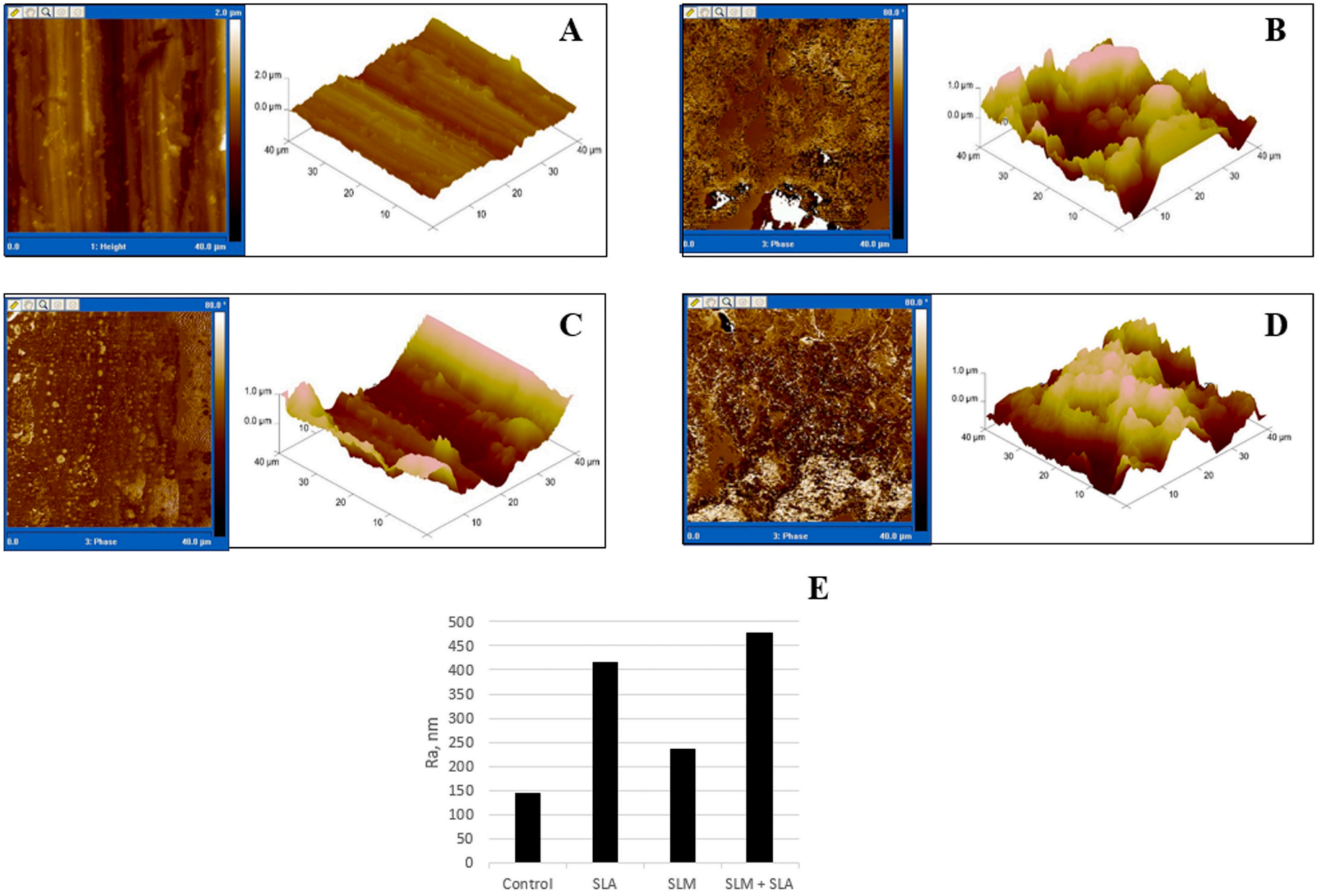

Fig. 2. The surface roughness of titanium alloy disks observed by using AFM. The images (40 × 40 µm) of the disks of a group 1 b group 2 c group 3, and d group 4 proved that surface topography differs significantly according to the nature of the technique. The highest surface roughness was witnessed in group 4.

Table 1
The chemical composition of the disks determined by EDX spectroscopy. Following the application of SLA or/and SLM techniques, the percentage of Ti, V, Al, and O on the surface of Ti6Al4V alloy disks was altered.

Group	Ti (%)	V (%)	Al (%)	O (%)
1	82.19	2.72	5.39	9.70
2	90.61	3.01	6.38	–
3	83.03	2.63	6.45	6.91
4	81.53	2.5	4.95	11.02

longitudinal parallel grooves and ridges due to the production of implants that came off the lathe, was encountered. The disks belonging to group 2 were treated using the SLA method, which created wide cavities and micropits on the surface. The SLM-treated disks in group 3 exhibited higher surface roughness than group 1. The application of both methods on the surface of the disks in group 4 resulted in a porous and irregular surface with the highest Ra value (477 nm) when compared with the surfaces of the other disks. EDX spectroscopy revealed that the ratio of V and Al slightly diminished, while the percentage of O_2 increased. The increased O_2 content was attributed to high Ti content, which binds oxygen upon oxidation [30]. In their report, Yang et al. [35] indicated that certain concentrations of O_2 added to pure titanium disks contributed to corrosion resistance and cell adhesion. The shortcoming of this part of our study is the number of disks analyzed for each group with AFM, SEM, EDX. Nevertheless, since we carried out SEM analysis in our initial work [17] and substantiated the former results in this study with the aforementioned approaches, we performed the analyses on only one disk in each group.

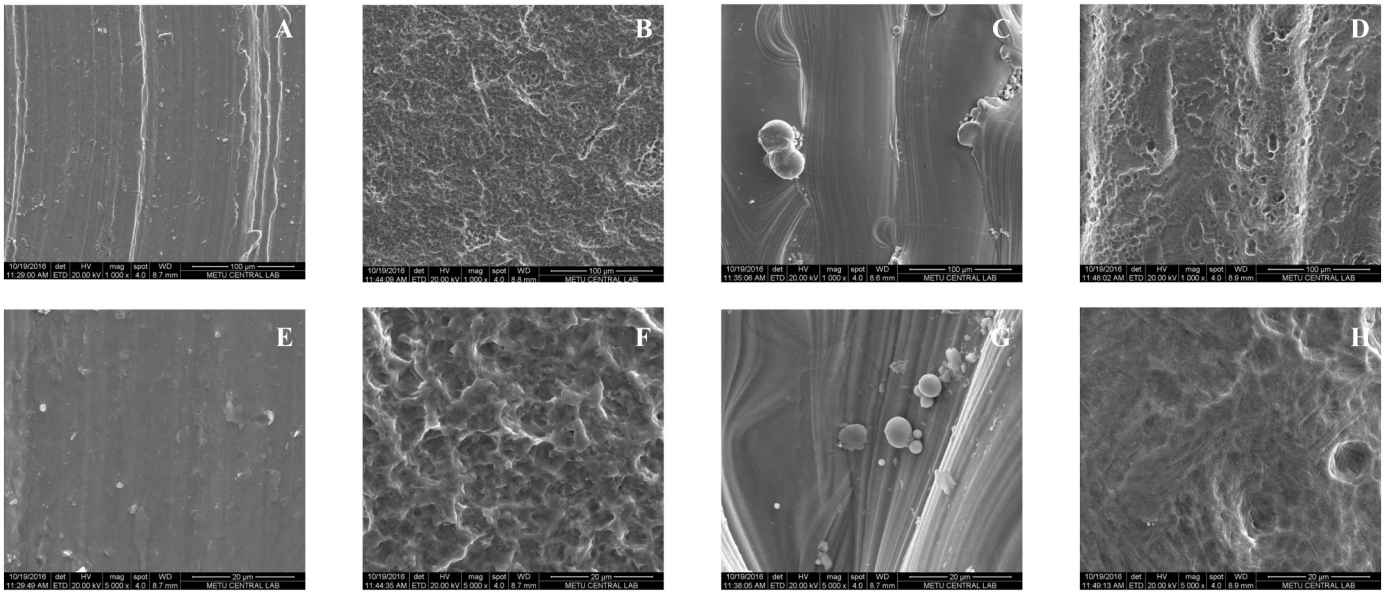

Fig. 3. SEM micro images of titanium disks with various surface properties. a, e control, b, f SLA, c, g SLM, d, h SLA+SLM, upper panel 1000× magnification, lower panel 5000× magnification.

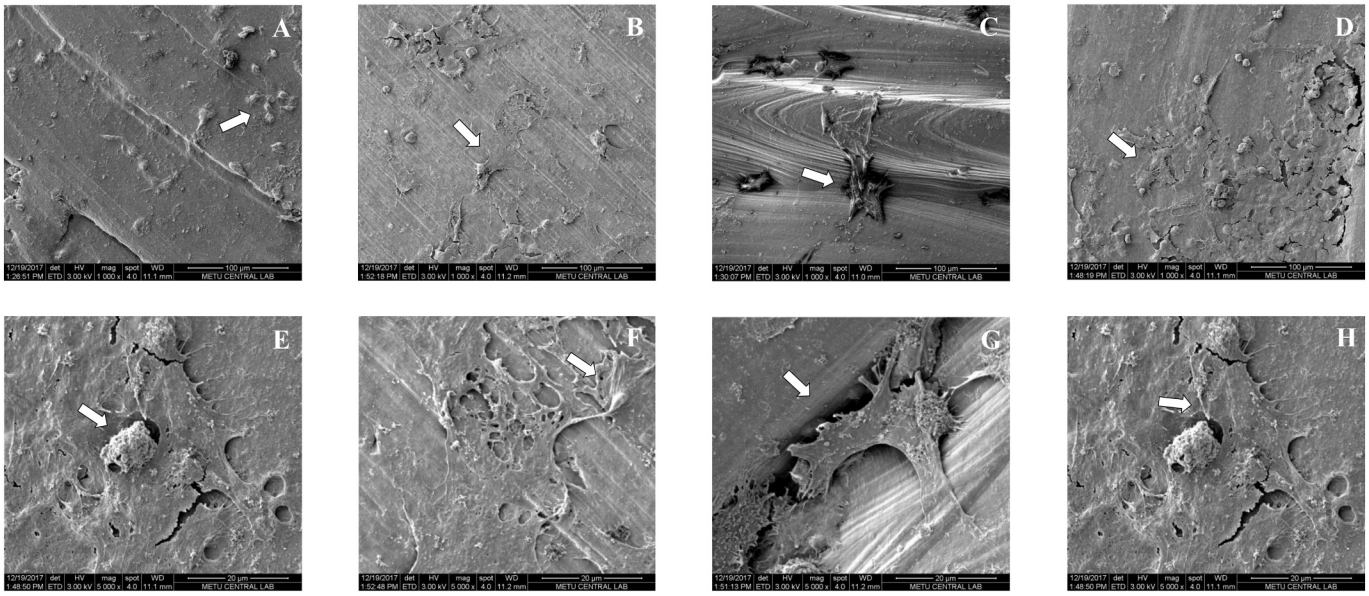

Fig. 4. The attachment of Saos-2 cells on the surface of titanium alloy disks evaluated by SEM imaging. The images captured on day 7 at a magnification of 1000× (upper panel) and 5000× (lower panel) represents a, e group 1, b, f group 2, c, g group 3, and d, h group 4. The white arrows highlight Saos-2 cells adhered to the surface alloy disks.

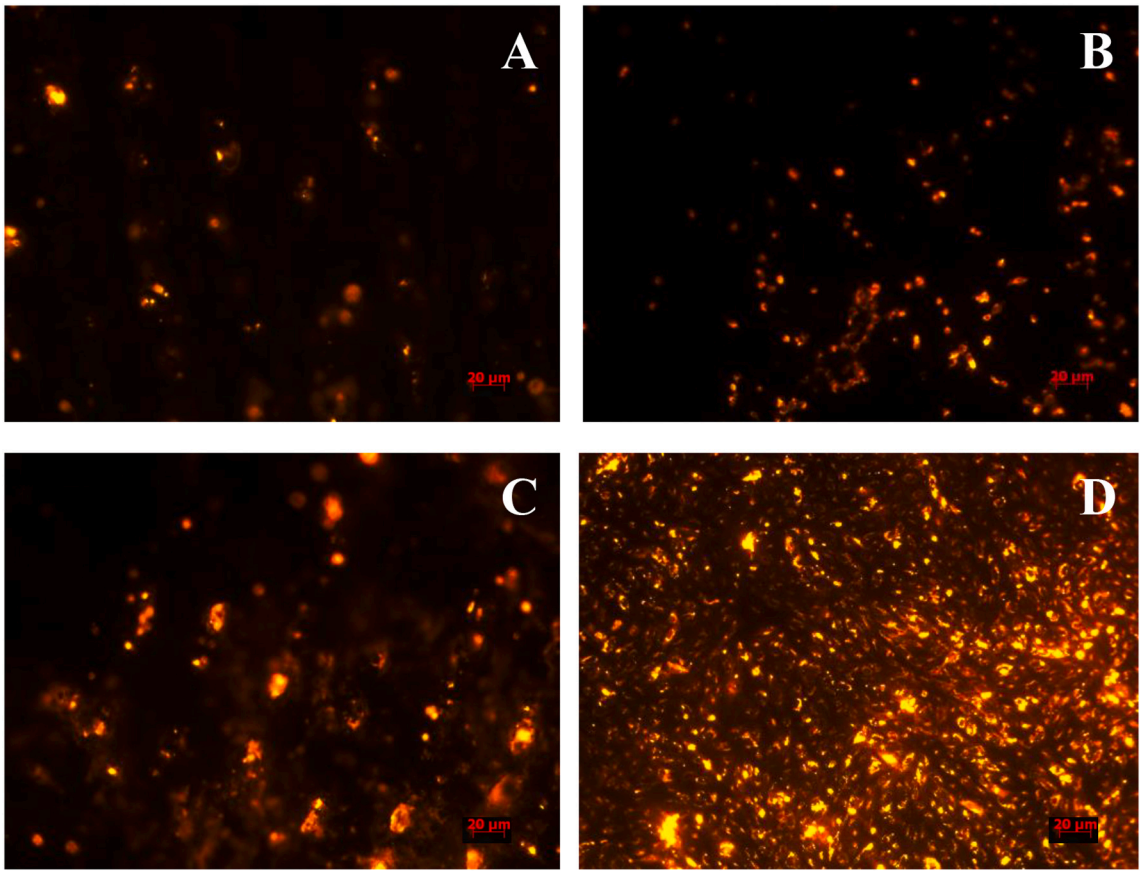

Fig. 5. Fluorescence imaging (10 X) of Dil-labeled Saos-2 cells attached on the surface of titanium alloy disks. The distinct surface roughness of the a untreated, b SLA-treated, c SLM-treated, and d SLM+SLA-treated disks affected the attachment and proliferation of the Saos-2 cells on the disks.

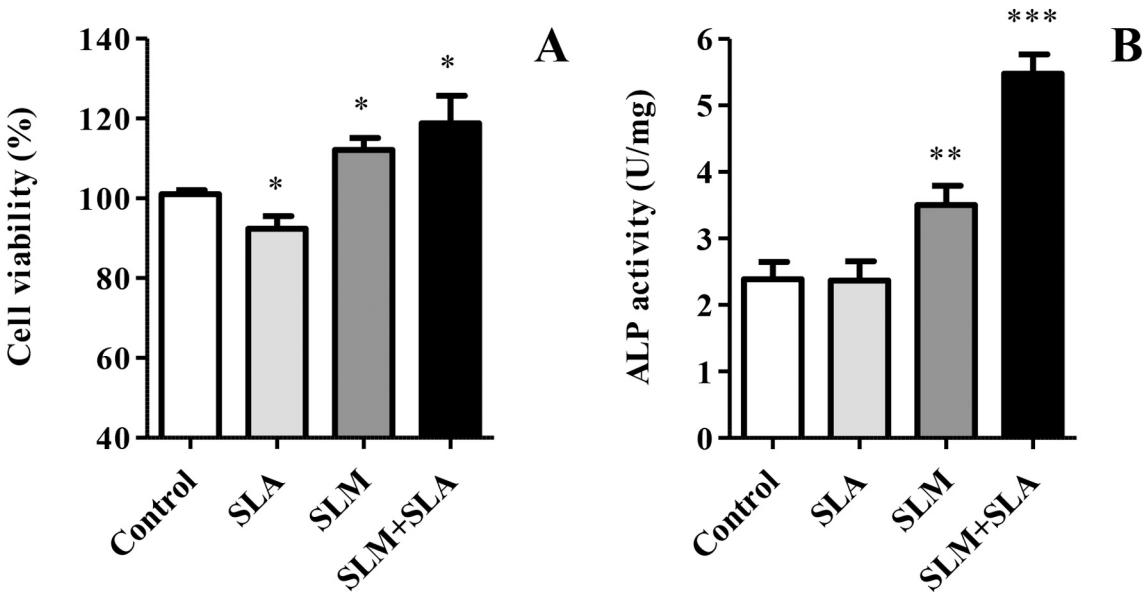

Fig. 6. MTT and ALP activity assay results of Saos-2 cells seeded onto titanium alloy disks with specific surface alterations and incubated for 72 h. a The metabolic activity of the Saos-2 cells suggested that the viable cell ratio was higher when the cells were planted onto Ti-6Al-4V alloy disks subjected to surface treatments that led to increased surface roughness in comparison to the viability of the cells seeded onto the relatively smoother surface of the group 1disk. b The ALP activity of Saos-2 cells was augmented when seeded onto those disks with higher Ra values when compared with the ALP activity of the cells proliferated on the untreated smooth disk surface ($n = 4 \pm$ SD; *$p < 0.05$, **$p < 0.01$, and ***$p < 0.001$ vs. control).

The dental implant must be compatible to interface with osteoblasts, epithelial cells and fibroblasts. Osteoblasts eventually generate bone tissue, while epithelial cells adhere to the dorsal side of the tissue and the implant, constituting a seal between them. Fibroblasts form a collagen-rich connective tissue and aid in the proper anchoring of the implant [36]. It was previously demonstrated that the surface topography and physicochemical characteristics of dental implants determine the behavior, morphology, and viability of cells and tissues [37].

In this study, we employed the Saos-2 human osteosarcoma cell line to investigate whether the implementation of SLA or/and SLM surface modification methods affect the viability, proliferation, and attachment of healthy cells on the titanium alloy disks. These adherent osteoblast-like cells displayed different morphology and behavior when seeded onto the titanium alloy disks of different groups. The group 3 and group 4 disks conferred a more effective surface for higher attachment and metabolic activity, according to the results of SEM analysis and MTT assay. Visualization of the labeled cells using fluorescent microscopy further revealed larger viable cell numbers on the surfaces of the disks treated with both SLM and SLA. It was concluded that increasing the surface Ra value provided a biocompatible topography where Saos-2 cells could proliferate appropriately.

An important factor underlying the biomechanical relationship between the implant and the bone is the determination of the basic shear stress between the implant and bone support by the amount of bone formed in the irregularities on the implant surface. ALP, along with various other compounds including calcium, osteopontin, osteocalcin [38], and type I collagen [39] is a marker of early osteoblastic differentiation and activity, since augmented levels of these molecules are encountered in bone formation. It was previously discovered that the ALP activity of Saos-2 cells is triggered upon the plantation of sand-blasted and titanium plasma-sprayed (TPS) dental implants [40]. The data of our study confirmed that SLA and SLM application on the surface of Ti6Al4V alloy disks coated with Ti6Al4V ELI alloy promoted the ALP activity of Saos-2 cells significantly, compared to the activity of the enzyme in the cells seeded onto disks belong to groups 1, 2, and 3. These results confirms that surface roughness is crucial for the osteoblast-like cells to adhere, proliferate, and differentiate on titanium dental implants, which is one of the major indicators of successful implantation.

5. Conclusion

1. The success or failure of dental implants surface is related not only to the chemical properties of the implant surface but also to its micro-morphological nature.
2. Ti6Al4V disks coated with Ti6Al4V ELI alloy and subjected to SLA demonstrated high surface roughness, which provided a favorable habitat for osteoblast-like Saos-2 cells to adhere to and proliferate. Moreover, metabolic activity, as well as ALP activity indicating osteoblastic differentiation, were intensified in the Saos-2 cells planted onto these disks.
3. Saos-2 cell adhesion increased on Ti6Al4V ELI alloy coated disks in direct proportion to the thickness of the TiO_2 layer. It can be predicted that this enhancement will shorten the osseointegration time and thus expedite the loading protocols. As the surface roughness surges to a certain level, the biological morphology of osteoblasts is positively affected, and cell adhesion and functional behavior increase.
4. The comparative assessment of different surface treatments revealed that SLM and SLA dual-treatment is a preferable mode of surface construction based on rough and irregular indentations of the titanium following the supplementary treatments.
5. Upon further studies, titanium implants treated with SLM+SLA dual surface modification may be upgraded for superior quality and used in the clinic not only for dental implants but also for orthopedics.

Abbreviations

3D	three-dimensional
AFM	atomic force microscope
ALP	alkaline phosphatase
ARD	anti-resorptive drug
ASTM	American Society for Testing and Materials
ATCC	American Type Culture Collection
CAD	computer-aided design
CNC	computer numerical control
DAE	dual-acid etching
DMEM	Dulbecco's Modified Eagle Medium
DMF	dimethylformamide
EDX	energy-dispersive x-ray spectroscopy
ELI	extra low interstitials
HMDS	hexamethyldisilazane
$NaHCO_3$	Sodium bicarbonate
pNPP	*p*-nitrophenyl phosphate
SDS	sodium dodecyl sulfate
SEM	Scanning Electron Microscope
SLA	sand-blasted, large-grit, acid-etching
SLM	selective laser melting
Ti6Al4V	Titanium-6-Aluminum-4-Vanadium
TPS	titanium plasma-sprayed
UV	ultraviolet

Fundings

This study was supported by Hacettepe University Scientific Research Unit (HÜBAB 11614).

Availability of data and materials

The datasets used and/or analyzed during this study are available from the corresponding author on request.

Ethics approval and consent to participate

Not applicable.

Consent for publication

All authors approved the final manuscript.

CRediT authorship contribution statement

EOO: Principal author. Constructed the titanium alloy disks and conducted the experiments. Wrote the manuscript. AE: Designed the in vitro studies and supervised the whole study. SO: Carried out certain experiments and wrote the manuscript. OA: Constructed the titanium alloy disks. BE: Corresponding author. Designed and supervised the whole study. EOO, AE, SO, and BE: Approved the submitted version of this study. All authors read and approved the final manuscript.

Declaration of competing interest

The authors declare that they have no competing interests.

Acknowledgements

Not applicable.

References

[1] M.S. Alrajhi, O. Askar, A.A. Habib, M.A. Elsyad, Maxillary bone resorption with conventional dentures and four-implant-supported fixed prosthesis opposed by

distal-extension partial dentures: a preliminary 5-year retrospective study, Int. J. Oral Maxillofac. Implants 35 (2020) 816–823.
[2] C.N. Elias, D.J. Fernandes, C.R. Resende, J. Roestel, Mechanical properties, surface morphology and stability of a modified commercially pure high strength titanium alloy for dental implants, Dent. Mater. 31 (2015) e1–e13.
[3] T. Albrektsson, P.I. Brånemark, H.-A. Hansson, B. Kasemo, K. Larsson, I. Lundström, D.H. McQueen, R. Skalak, The interface zone of inorganic implantsIn vivo: titanium implants in bone, Ann. Biomed. Eng. 11 (1983) 1–27.
[4] H.S. Alghamdi, Methods to improve osseointegration of dental implants in low quality (type-IV) bone: an overview, J. Funct. Biomater. 9 (2018).
[5] E. Pérez-Pevida, A. Brizuela-Velasco, D. Chávarri-Prado, A. Jiménez-Garrudo, F. Sánchez-Lasheras, E. Solaberrieta-Méndez, M. Diéguez-Pereira, F.J. Fernández-González, B. Dehesa-Ibarra, F. Monticelli, Biomechanical consequences of the elastic properties of dental implant alloys on the supporting bone: finite element analysis. Biomed. Res. Int., 2016 (2016) 1850401.
[6] F. Schwarz, M. Langer, T. Hagena, B. Hartig, R. Sader, J. Becker, Cytotoxicity and proinflammatory effects of titanium and zirconia particles, Int. J. Implant. Dent. 5 (2019) 25.
[7] J.Y. Kim, H. Choi, J.H. Park, H.D. Jung, Y.S. Jung, Effects of anti-resorptive drugs on implant survival and peri-implantitis in patients with existing osseointegrated dental implants: a retrospective cohort study, Osteoporos. Int. 31 (2020) 1749–1758.
[8] A.E. Hakam, G. Vila, P.M. Duarte, M.P. Mbadu, D.S. Ai Angary, H. Shuwaikan, I. Aukhil, R. Neiva, H.D.P. da Silva, J. Chang, Effects of different antidepressant classes on dental implant failure: a retrospective clinical study, J. Periodontol. 92 (2021) 196–204.
[9] M. Rahmati, S.P. Lyngstadaas, J.E. Reseland, I. Andersbakken, H.S. Haugland, M. López-Peña, A.G. Cantalapiedra, F.M. Guzon Muñoz, H.J. Haugen, Coating doxycycline on titanium-based implants: two in vivo studies, Bioact. Mater. 5 (2020) 787–797.
[10] Z. Hu, X. Wang, W. Xia, Z. Wang, P. Zhang, L. Xia, K. Lin, M. Zhu, Nano-structure designing promotion osseointegration of hydroxyapatite coated Ti-6Al-4V alloy implants in diabetic model, J. Biomed. Nanotechnol. 15 (2019) 1701–1713.
[11] S. Zhang, X. Lin, J. Chen, W. Huang, Chin. Effect of solution temperature and cooling rate on microstructure and mechanical properties of laser solid forming Ti-6Al-4V alloy. Opt. Lett., 7 (2009) 498–501.
[12] M.A. Imam, C.M. Gilmore, Fatigue and microstructural properties of quenched Ti-6Al-4V, Metall. Trans. A. 14 (1983) 233–240.
[13] M.L. Lourenço, G.C. Cardoso, K. Sousa, T.A.G. Donato, F.M.L. Pontes, C. R. Grandini, Development of novel Ti-Mo-Mn alloys for biomedical applications, Sci. Rep. 10 (2020) 6298.
[14] H. Galarraga, D.A. Lados, R.R. Dehoff, M.M. Kirka, P. Nandwana, Effects of the microstructure and porosity on properties of Ti-6Al-4V ELI alloy fabricated by electron beam melting (EBM), Addit. Manuf. 10 (2016) 47–57.
[15] M. Khandaker, S. Riahinezhad, Y. Li, M.B. Vaughan, F. Sultana, T.L. Morris, L. Phinney, K. Hossain, Plasma nitriding of titanium alloy: effect of roughness, hardness, biocompatibility, and bonding with bone cement, Biomed. Mater. Eng. 27 (2016) 461–474.
[16] A. Szyszkowski, M. Kozakiewicz, Effect of implant-abutment connection type on bone around dental implants in long-term observation: internal cone versus internal hex, Implant Dent. 28 (2019) 430–436.
[17] O. Arifagaoglu, S. Oncul, A. Ercan, O. Olcay, B. Ersu, HGF-1 proliferation on titanium dental implants treated with laser melting technology, Niger. J. Clin. Pract. 22 (2019) 251–257.
[18] N. Otawa, T. Sumida, H. Kitagaki, K. Sasaki, S. Fujibayashi, M. Takemoto, T. Nakamura, T. Yamada, Y. Mori, T. Matsushita, Custom-made titanium devices as membranes for bone augmentation in implant treatment: modeling accuracy of titanium products constructed with selective laser melting, J. Craniomaxillofac. Surg. 43 (2015) 1289–1295.
[19] F.J. van Velzen, R. Ofec, E.A. Schulten, C.M. Ten Bruggenkate, 10-year survival rate and the incidence of peri-implant disease of 374 titanium dental implants with a SLA surface: a prospective cohort study in 177 fully and partially edentulous patients, Clin. Oral Implants Res. 26 (2015) 1121–1128.
[20] M. Menini, E. Dellepiane, D. Baldi, M.G. Longobardi, P. Pera, A. Izzotti, Microarray expression in peri-implant tissue next to different titanium implant surfaces predicts clinical outcomes: a split-mouth study, Clin. Oral Implants Res. 28 (2017) e121–e134.
[21] W.A. Camargo, S. Takemoto, J.W. Hoekstra, S.C.G. Leeuwenburgh, J.A. Jansen, J. van den Beucken, H.S. Alghamdi, Effect of surface alkali-based treatment of titanium implants on ability to promote in vitro mineralization and in vivo bone formation, Acta Biomater. 57 (2017) 511–523.
[22] M. Katschnig, J. Wallner, T. Janics, C. Burgstaller, W. Zemann, C. Holzer, Biofunctional glycol-modified polyethylene terephthalate and thermoplastic polyurethane implants by extrusion-based additive manufacturing for medical 3D maxillofacial defect reconstruction, Polymers (Basel) 12 (2020).
[23] M. Özcan, C. Hämmerle, Titanium as a reconstruction and implant material in dentistry: advantages and pitfalls, Materials 5 (2012) 1528–1545.
[24] G. Asensio, B. Vázquez-Lasa, L. Rojo, Achievements in the topographic design of commercial titanium dental implants: towards anti-peri-implantitis surfaces, J. Clin. Med. 8 (2019).
[25] F.N. Barrak, S. Li, A.M. Muntane, J.R. Jones, Particle release from implantoplasty of dental implants and impact on cells, Int. J. Implant. Dent. 6 (2020) 50.
[26] J.G.S. Souza, C.V. Lima, B.E. Costa Oliveira, A.P. Ricomini-Filho, M. Faveri, C. Sukotjo, M. Feres, A.A. Del Bel Cury, V.A.R. Barão, Biofouling, Dose-response effect of chlorhexidine on a multispecies oral biofilm formed on pure titanium and on a titanium-zirconium alloy. 34 (2018) 1175–1184.
[27] Z. Berryman, L. Bridger, H.M. Hussaini, A.M. Rich, M. Atieh, A. Tawse-Smith, Titanium particles: an emerging risk factor for peri-implant bone loss, Saudi Dent. J. 32 (2020) 283–292.
[28] S. Szmukler-Moncler, C. Blus, D. Morales Schwarz, G. Orrù, Characterization of a macro- and micro-textured titanium grade 5 alloy surface obtained by etching only without sandblasting, Materials (Basel) 13 (2020).
[29] K.-Y. Hung, S.-C. Lo, C.-S. Shih, Y.-C. Yang, H.-P. Feng, Y.-C. Lin, Titanium surface modified by hydroxyapatite coating for dental implants, Surf. Coat. Technol. 231 (2013) 337–345.
[30] S.A. Cho, S.K. Jung, A removal torque of the laser-treated titanium implants in rabbit tibia, Biomaterials 24 (2003) 4859–4863.
[31] D.L. Cochran, D. Buser, C.M. ten Bruggenkate, D. Weingart, T.M. Taylor, J. P. Bernard, F. Peters, J.P. Simpson, The use of reduced healing times on ITI implants with a sandblasted and acid-etched (SLA) surface: early results from clinical trials on ITI SLA implants, Clin. Oral Implants Res. 13 (2002) 144–153.
[32] I. Yadroitsev, L. Thivillon, P. Bertrand, I. Smurov, Strategy of manufacturing components with designed internal structure by selective laser melting of metallic powder, Appl. Surf. Sci. 254 (2007) 980–983.
[33] T. Bormann, R. Schumacher, B. Müller, M. Mertmann, M. de Wild, Tailoring selective laser melting process parameters for NiTi implants, J. Mater. Eng. Perform. 21 (2012) 2519–2524.
[34] Z.J. Wally, A.M. Haque, A. Feteira, F. Claeyssens, R. Goodall, G.C. Reilly, J Mech Selective laser melting processed Ti6Al4V lattices with graded porosities for dental applications, Behav. Biomed. Mater. 90 (2019) 20–29.
[35] C.H. Yang, Y.T. Wang, W.F. Tsai, C.F. Ai, M.C. Lin, H.H. Huang, Effect of oxygen plasma immersion ion implantation treatment on corrosion resistance and cell adhesion of titanium surface, Clin. Oral Implants Res. 22 (2011) 1426–1432.
[36] D.W. Hamilton, B. Chehroudi, D.M. Brunette, Comparative response of epithelial cells and osteoblasts to microfabricated tapered pit topographies in vitro and in vivo, Biomaterials 28 (2007) 2281–2293.
[37] D.C. Krishnadath, W. Ruan, H. Yang, J. Liu, X. Zhou, Influence of low modulus Co-Zr alloys surface modification on protein adsorption and MC3T3-E1, NIH3T3 and RAW264.7 cell behaviour, J. Biomater. Appl. 35 (2021) 1061–1070.
[38] X. Han, N. Zhu, Y. Wang, G. Cheng, 1,25(OH)2D3 inhibits osteogenic differentiation through activating β-catenin signaling via downregulating bone morphogenetic protein 2, Mol. Med. Rep. 22 (2020) 5023–5032.
[39] J. Zheng, X. Zhu, Y. He, S. Hou, T. Liu, K. Zhi, T. Hou, L. Gao, CircCDK8 regulates osteogenic differentiation and apoptosis of PDLSCs by inducing ER stress/ autophagy during hypoxia. Ann N Y Acad Sci, 1485 (2021) 56–70.
[40] L. Postiglione, G. Di Domenico, L. Ramaglia, S. Montagnani, S. Salzano, F. Di Meglio, L. Sbordone, M. Vitale, G. Rossi, Behavior of SaOS-2 cells cultured on different titanium surfaces, J. Dent. Res. 82 (2003) 692–696.